Formation of antihydrogen by the charge-transfer reaction

J. Mitroy
Faculty of Science, Northern Territory University, Casuarina, NT, 0909, Australia
(Received 2 March 1995)

The cross sections for antihydrogen formation in the $n=1$, 2, 3, 4, 5, 6, and 7 levels from antiproton-positronium collisions are computed in the unitarized Born approximation (UBA). Twenty-seven physical states of antihydrogen ($1s \rightarrow 7h$) and ten physical states ($1s \rightarrow 4f$) of positronium are included in the UBA basis. The peak cross section for antihydrogen formation from excited positronium targets is much larger than that from a ground-state positronium target at low incident energies. The high-n antihydrogen levels make a significant contribution to the total antihydrogen formation cross section, especially for incident positronium atoms in the Ps($n=3$) and Ps($n=4$) levels.

PACS number(s): 34.90.+q, 34.80.Dp, 36.10.Dr

I. INTRODUCTION

When the antihydrogen atom is isolated from ordinary matter it is stable and is consequently the ideal system in which to study the charge-conjugation symmetries of physics [1–3]. Other exotic atoms such as muonium, positronium, and protonium have short lifetimes and are not so suitable for high-precision spectroscopic studies. Given the availability of a suitable antiproton beam from the low-energy antiproton ring at CERN, experiments designed to produce and study antihydrogen atoms are being developed [3–7].

One of the factors that influences the viability of any experiment is, of course, the rate at which antihydrogen can be formed. One of the most promising methods that has been suggested for producing antihydrogen [5–7] is to use the charge-exchange process

$$\mathrm{Ps}+\bar{p}\rightarrow e^{-}+\bar{\mathrm{H}}.$$

The cross section for antihydrogen formation by this reaction is larger than the cross section via a number of alternative reactions [3]. The specific configuration of one proposed experiment is as follows [7]. A large number of antiprotons are stored in a cryogenic Penning trap. A positron beam is directed onto the walls of the ion trap. A small fraction of the positron beam will then combine with electrons to form positronium atoms, which then drift into the trap. These positronium atoms then collide with antiprotons to form antihydrogen. There have been relatively few calculations of the charge-transfer process leading to antihydrogen formation. Humberston *et al.* [8] combined accurate variational calculations in the Ore gap with distorted-wave calculations to estimate the cross section for ground-state antihydrogen formation. The close-coupling method [9,10] has also been used to compute cross sections for antihydrogen formation to the $\bar{\mathrm{H}}(1s)$, $\bar{\mathrm{H}}(2s)$, and $\bar{\mathrm{H}}(2p)$ levels from the Ps ground state in a six-state model for incident positronium energies from 0 to 54 eV. It was found that the charge-transfer cross section should peak around $14\pi a_0^2$ for incident positronium energies of 5–10 eV. A more accurate calculation using a mixed physical and pseudostate basis was recently carried out [11] in the energy region below the ionization threshold. Besides computing the integral cross section from the positronium ground state, differential cross sections were also computed [11] so that the recoil conditions appropriate to the collision could also be determined. Another very recent calculation was the hyperspherical close-coupling calculation of Igarashi, Toshima, and Shirai [12]. The cross sections from this model are expected to be of similar accuracy to those of Mitroy and Ratnavelu [11] for the ground state.

The rate at which antihydrogen is formed can be enhanced if lasers are used to pump positronium into highly excited levels, since the cross section for the reaction

$$\mathrm{Ps}(ml)+\bar{p}\rightarrow e^{-}+\bar{\mathrm{H}}(nl')$$

is larger than the cross section from the positronium ground state. In order to avoid possible confusion, the principal quantum number for a positronium Rydberg level is denoted by m, and that for an antihydrogen level is written as n. According to semiclassical theory, the charge-transfer cross sections are expected to scale as m^4 for positronium atoms in a Rydberg level [13]. Two calculations of antihydrogen formation from excited positronium states have been done with the first Born approximation [14,15]. These calculations were performed at relatively high energies where the particle-transfer cross sections for Ps atoms in an initial Rydberg level scale as m^{-3}. However, at low energies the charge-transfer cross section is greatly enhanced for excited positronium atoms. Mitroy and Stelbovics [16] coupled six hydrogen and three positronium levels in the unitarized Born approximation (UBA) to demonstrate that the charge-transfer cross section for antihydrogen formation could increase by an order of magnitude at the cross-section peak if the incident positronium atom was initially in an $m=2$ level. This result was subsequently confirmed by the hyperspherical coupled-channel (CC) calculations [12]. The qualitative features of the UBA and hyperspherical CC cross sections are roughly the same, despite some differences in detail. It is expected that the hyperspherical CC calculations will give more accurate cross sections than the UBA.

In this work, the earlier UBA calculations [16] are extended to incorporate a much larger channel space. Positronium states up to the $m=4$ level and antihydrogen states up to the $n=7$ level (excluding the $7i$ level) were included in the basis. The calculations are performed using the UBA. The UBA is not as accurate as the close-coupling method, but it corrects the most glaring deficiency of the first Born approximation (lack of unitarity) and should be sufficiently accurate for an initial survey to investigate (a) how the cross section scales for increasing m, (b) the fractionation of the antihydrogen atoms into different levels, and (c) the energy dependence of the cross section.

II. DETAILS OF THE CALCULATION

Cross sections for antihydrogen production from the Ps($1s$), Ps($2s$) and Ps($2p$), Ps($3s$), Ps($3p$), and Ps($3d$), Ps($4s$), Ps($4p$), Ps($4d$), and Ps($4f$) states to the antihydrogen ground and excited states are computed. The calculations use a 37-state ($\bar{\mathrm{H}}(n=1, 2, 3, 4, 5, 6, 7)$, Ps($m=1, 2, 3, 4$)) unitarized Born approximation (the $7i$ level was not included in the explicit calculation). The unitarized Born approximation (UBA) is the first Born approximation to the K matrix. Using the notation that hydrogen states are labeled by the subscripts α and α' and positronium states are labeled by the subscripts β and β', the on-shell UBA equations are

$$\langle \mathbf{k}'\Psi_{\alpha'}|T|\mathbf{k}\Psi_{\alpha}\rangle = \langle \mathbf{k}'\Psi_{\alpha'}|V|\mathbf{k}\Psi_{\alpha}\rangle - \sum_{\alpha''} i\pi k'' \int d\hat{\mathbf{k}}''\langle \mathbf{k}'\Psi_{\alpha'}|V|\mathbf{k}''\Psi_{\alpha'}\rangle\langle \mathbf{k}''\Psi_{\alpha'}|T|\mathbf{k}\Psi_{\alpha}\rangle$$
$$- \sum_{\beta''} i2\pi k'' \int d\hat{\mathbf{k}}''\langle \mathbf{k}'\Psi_{\alpha'}|V|\mathbf{k}''\Phi_{\beta'}\rangle\langle \mathbf{k}''\Phi_{\beta''}|T|\mathbf{k}\Psi_{\alpha}\rangle$$

$$\langle \mathbf{k}'\Phi_{\beta'}|T|\mathbf{k}\Psi_{\alpha}\rangle = \langle \mathbf{k}'\Phi_{\beta'}|V|\mathbf{k}\Psi_{\alpha}\rangle - \sum_{\alpha''} i\pi k'' \int d\hat{\mathbf{k}}''\langle \mathbf{k}'\Phi_{\beta'}|V|\mathbf{k}''\Psi_{\alpha''}\rangle\langle \mathbf{k}''\Psi_{\alpha''}|T|\mathbf{k}\Psi_{\alpha}\rangle$$
$$- \sum_{\beta''} i2\pi k'' \int d\hat{\mathbf{k}}''\langle \mathbf{k}'\Phi_{\beta'}|V|\mathbf{k}''\Phi_{\beta''}\rangle\langle \mathbf{k}''\Phi_{\beta''}|T|\mathbf{k}\Psi_{\alpha}\rangle .$$

The generic term V is used to label the interaction between the different classes of channels. The momenta $\mathbf{k}$, $\mathbf{k}'$, and $\mathbf{k}''$ are restricted to be equal to the on-shell momenta of the different entrance and exit channels. Once the K matrix is computed, it is then converted to the T matrix and the cross section is computed.

Partial cross sections were explicity computed up to a maximum partial-wave angular momentum of 36. The large number of partial waves was motivated by the need to get converged cross sections for Ps($m=4$) initial states. At the lowest energies a converged cross section could be obtained by summing fewer partial waves. The partial-wave sum was extrapolated to infinite J by assuming that the partial cross sections scale like a power series. The size of the correction made to the cross section by this extrapolation was generally less than 5%. The calculations utilized a recently derived expression for the rearrangement matrix element [17]. Since a $7i$ level was not included in the explicit calculation, a cross section for this state was incorporated by assuming the cross sections to the $7i$ state were the same as those to the $7h$ level.

All of the actual cross sections shown later included a correction arising from the need to include contributions from positron transfer to the $\bar{\mathrm{H}}(n=8)$ and higher levels. The relative size of this correction was largest for Ps($m=4$) initial states and smallest for the Ps($1s$) initial state. The actual procedure used to estimate the cross section for these higher Rydberg levels was obtained from the cross section to the $n=7$ level by

$$\sigma(n>7) = (7/n)^3 (E_n/E_7)^{1/2} \sigma(n=7).$$

The first term of this formula is based upon $1/n^3$ scaling for the positronium formation matrix element. The second factor involving the ratio of the outgoing electron energies after the charge-transfer process has occurred (E_n and E_7 for transfer to the nth and 7th antihydrogen levels, respectively), is based upon kinematic considerations [a factor of $(E_f/E_i)^{1/2}$ is present when the square of the T matrix is converted to the cross section] and only affects the extrapolation close to

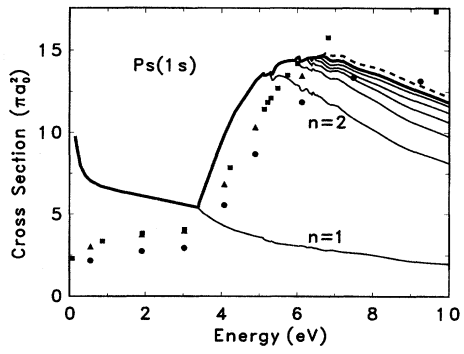

FIG. 1. Cross sections for antihydrogen formation (in πa_0^2) from the Ps($1s$) ground state. The positronium energy is given in eV. The series of curves shows the accumulated antihydrogen cross section for the $n=1$, 2, 3, 4, 5, 6, and 7 levels. The dashed curve includes a correction for higher-n levels obtained using n^{-3} scaling, as described in the text. Also shown are the cross sections from six-state (●) [9] and twelve-state (▲) [11] close-coupling calculations, and the hyperspherical calculation (■) [12].

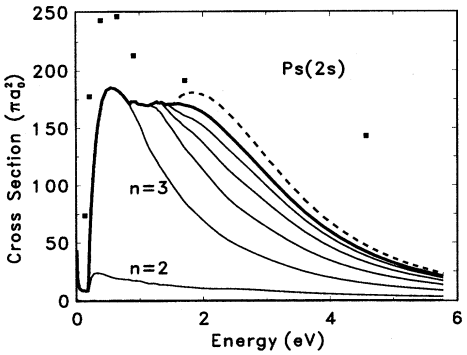

FIG. 2. Cross sections for antihydrogen formation (in πa_0^2) from the Ps($2s$) level. The details of the present UBA cross sections are the same as Fig. 1. Cross sections from the hyperspherical calculation (■) [12] are also shown.

threshold. This formula was used to estimate corrections from the $n=8$ to the $n=14$ levels, which were then added to the cross section.

The cross sections are shown for incident energies [in the Ps($1s$)-p channel] of less than 10 eV since the main interest is at low energies where the cross section is largest. Given that the calculations involve the explicit calculation of UBA T-matrices at about 100 energies for transition arrays containing up to 37 initial and final states, it is not possible to present the massive amount of information in tabular form. All the cross sections are presented in graphical form. Prior to graphing, the cross-section arrays were organized by using a commercial spreadsheet computer program (Borland Quattro-Pro 5.0) with three-dimensional capabilities. The cross sections that are reported for initial positronium states with $l>0$ are computed assuming that each individual magnetic sublevel of the target level is equally likely to be populated.

III. CROSS SECTIONS

The cross sections for antihydrogen production from the positronium ground state into all the possible levels are depicted as a function of energy in Fig. 1. The total cross section for the positron-transfer reaction is shown as a series of curves depicting the accumulated sum of the antihydrogen formation cross section for the $n=1,2,3,\ldots$ levels successively. An indication of the accuracy of the UBA calculation can be gained by the comparison with the six-state and twelve-state close-coupling cross sections. Distinctions exist between the UBA and CC cross sections; however, the magnitude of the cross-section maximum is the correct size and the shape is roughly correct. At the highest energy considered, the $\bar{H}(n>2)$ cross sections make up about 40% of the total integrated cross section. This would indicate that the earlier six-state CC calculation by Mitroy and Stelbovics [9,10] probably underestimates the antihydrogen cross section at energies above the ionization threshold. The twelve-state CC [11] and hyperspherical cross sections [12] are almost identical for energies below the $\bar{H}(n=3)$ threshold.

Cross sections for antihydrogen production from positronium in an excited $2s$ or $2p$ state are shown in Figs. 2 and 3. The cross section for antihydrogen formation in its ground state is insignificant for all practical purposes. Since the Ps($m=2$) levels and the H($n=3$) levels have similar binding energies and spatial extents, it is not surprising that the $\bar{H}(n=3)$ cross section is the single largest cross section. However, this cross section does not dominate the total cross section and at energies higher than 2.5 eV, and antihydrogen formation in the $\bar{H}(n=4)$ and higher levels accounts for

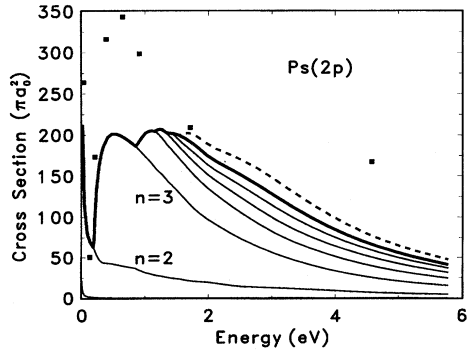

FIG. 3. Cross sections for antihydrogen formation (in πa_0^2) from the Ps($2p$) level. The details of the present UBA cross sections are the same as Fig. 2. Cross sections from the hyperspherical calculation (■) [12] are also shown.

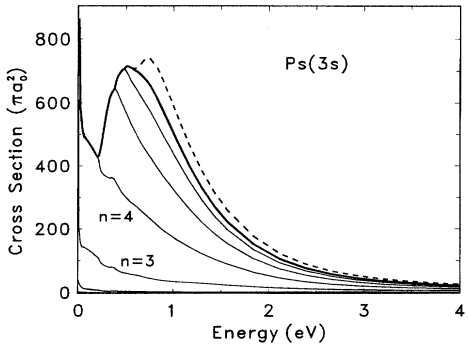

FIG. 4. Cross sections for antihydrogen formation (in πa_0^2) from the Ps($3s$) level. The details of the UBA cross sections are the same as Fig. 1.

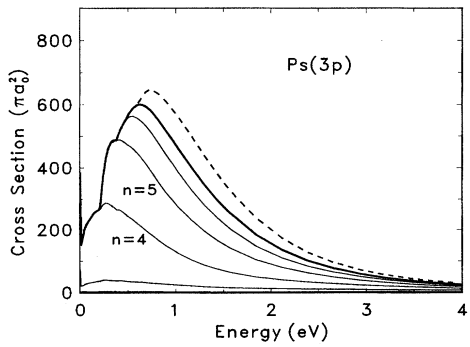

FIG. 5. Cross sections for antihydrogen formation (in πa_0^2) from the Ps($3p$) level. The details of the UBA cross sections are the same as Fig. 1.

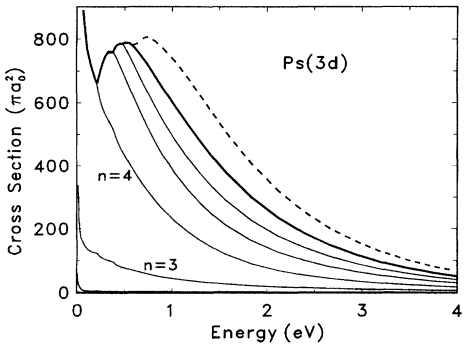

FIG. 6. Cross sections for antihydrogen formation (in πa_0^2) from the Ps($3d$) level. The details of the UBA cross sections are the same as Fig. 1.

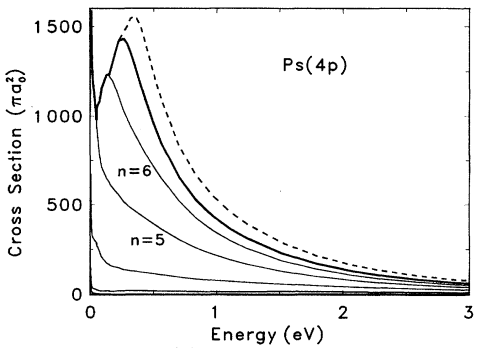

FIG. 8. Cross sections for antihydrogen formation (in πa_0^2) from the Ps($4p$) level. The details of the UBA cross sections are the same as Fig. 1.

more than half of the antihydrogen formation cross section. The UBA cross sections computed by Mitroy and Stelbovics [17] only included the $\bar{H}(n=3)$ states, and as a consequence, overestimate the rate at which the total antihydrogen cross section decreases as a function of energy. Although the present cross sections with the inclusion of the $\bar{H}$ levels with $n>3$ are in better agreement with the hyperspherical cross sections [12], there are still differences. First, the UBA predicts peak cross sections that are smaller. Second, as the energy increases the UBA cross sections decrease more rapidly than the hyperspherical cross sections.

The cross sections for Ps($3s$), Ps($3p$), and Ps($3d$) initial states are shown in Figs. 4–6, respectively. The cross section from the Ps($3d$) level has the highest peak cross section, and also decreases slower than the other two $m=3$ cross sections as the energy increases. Antihydrogen is predominantly formed in the $\bar{H}(n=3, 4, 5,$ and $6)$ levels, but the levels with $n\geq 7$ become increasingly important at higher energies and at 2 eV comprise 40% of the total antihydrogen cross section from the Ps($3d$) state.

The cross sections for the Ps($4s$), Ps($4p$), Ps($4d$), and Ps($4f$) initial states are shown in Figs. 7–10, respectively. The cross section from the Ps($4f$) level has the highest peak cross section of about $1890\pi a_0^2$. The positron-transfer cross section is generally dominated by $\bar{H}$ formation in the 5, 6, and 7 levels. Given the large size of the $n=7$ cross sections, it would have been preferable to include the $n=8$ levels explicitly in the calculation. However, the present calculation was the limit that could be done with the available computer resources levels and the current computer program. The correction factor for the higher $n=8-14$ levels does provide some sort of an estimate for the cross section to the missing levels, and a visual inspection of Figs. 7–10 seems to indicate no obvious problems with the correction. (The correction is probably most reliable at high energies and least reliable at low energies.) An examination of the cross section for the Ps($2p$), Ps($3d$), and Ps($4f$) initial states reveals that the cross-section maxima for these states are larger than those other Ps states with the same principal quantum number. The positronium levels with $m=l+1$ seem to result in the largest cross sections for antihydrogen formation.

There are two different energy regions where the antihydrogen formation from excited Ps states attain their maximum values. First, at very low energies, the charge-exchange cross sections follow a $E^{-1/2}$ energy dependence. This is merely a reflection of the fact that the cross section for superelastic scattering can diverge like $E^{-1/2}$ in the threshold region. The UBA cross sections should not be expected to give a particularly reliable estimate of the cross section in this region. Second, there is the local maximum (or maxima)

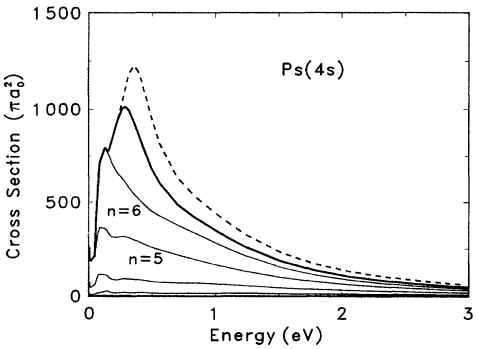

FIG. 7. Cross sections for antihydrogen formation (in πa_0^2) from the Ps($4s$) level. The details of the UBA cross sections are the same as Fig. 1.

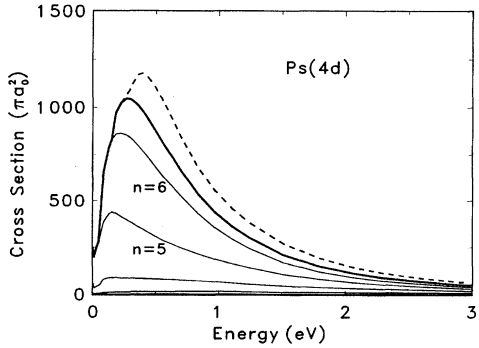

FIG. 9. Cross sections for antihydrogen formation (in πa_0^2) from the Ps($4d$) level. The details of the UBA cross sections are the same as Fig. 1.

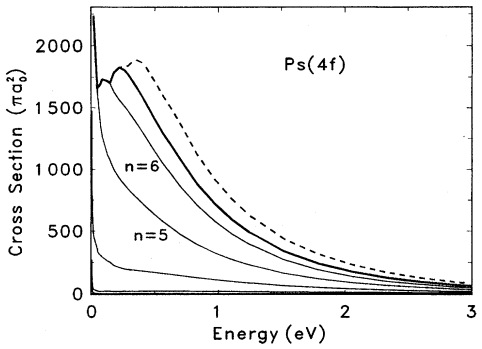

FIG. 10. Cross sections for antihydrogen formation (in πa_0^2) from the Ps($4f$) level. The details of the UBA cross sections are the same as Fig. 1.

in the cross section, occurring at roughly 6, 1, 0.7, and 0.4 eV, respectively, for Ps($m=1$), Ps($m=2$), Ps($m=3$), and Ps($m=4$), respectively. Experience with comparisons between close coupling and UBA calculations for electron scattering [18,19], and with the hyperspherical cross sections [12], would indicate that the cross section at the maximum is probably accurate to about 50%. The inclusion of the higher-n antihydrogen final states in the coupling scheme often results in giving the cross section a number of subsidiary maximum and delays the decrease in the cross section. In Table I, the energies at which the cross sections reach their maxima (given the complicated functional shapes of the cross sections, this is just an estimate), the cross sections at these energies, and the energies at which the cross sections decrease to half the maximum cross section are tabulated. A comparison of the peak cross sections for the Ps($m=2$, 3, and 4) initial states appear to indicate the peak cross section scales as m^3, not m^4 as suggested by Charlton [13]. There is some uncertainty regarding the contribution from the $\bar{\text{H}}$ levels with $n \geq 8$. However, it is unlikely that explicit inclusion of the $\bar{\text{H}}(n \geq 8)$ levels into the calculation would lead to a sufficiently large change in the antihydrogen cross section near the cross-section peak to support an m^4 law. There is another factor that could prevent the laser excitation of the Ps atoms in an ion trap, resulting in the maximum possible antihydrogen formation rate. The energy range over which the cross section is large gets smaller as the quantum number of the positronium initial state increases. Consequently, the antihydrogen formation rate could be reduced if the thermal distribution of the positronium atoms in the trap has a larger energy spread than the region over which the positron-transfer cross section is large. In such circumstances, it would be desirable to decrease the thermal energy of the positronium atoms, and schemes for doing this do exist [20,21].

IV. CONCLUSIONS

A number of conclusions can be drawn from the cross sections reported in this work. First, the peak cross section for antihydrogen is generally bigger for higher m positronium initial states. Based on the available evidence, the scaling law that seems to describe the increase in cross sections is an m^3 law, and not an m^4 law. Second, the width of the energy region over which the cross section is large gets narrower as the quantum number of the positronium target atom increases. These two conclusions must be qualified to some extent; the hyperspherical calculation gave cross sections that had a larger peak and did not decrease as rapidly as the energy increased. Third, after the positron transfer, a wide variety of antihydrogen states will be populated, including some high-n levels. The population of these higher-n levels results in a broader energy region where the cross section is large. Fourth, some of the calculations predict larger cross sections that diverge like $E^{-1/2}$ as the relative energy of the positronium-proton system goes to zero. However, the numerical predictions of the UBA at these energies just above the positronium thresholds are probably reliable only to an order of magnitude.

Taken as a whole, the present calculations provide further evidence to support the use of laser excitation in order to increase antihydrogen production. However, two of the factors mentioned above could act to partially negate the optimistic predictions [7,13] of greatly enhanced antihydrogen production. These are the apparent scaling of the antihydrogen cross section in terms of the positronium principal quantum number as a function of m^3, and the decreasing energy width of the region where the cross section is large. If the temperature of the positronium atoms formed in an ion trap is about 1 eV, then it is entirely possible that the gain in production from the larger cross section from a highly excited positronium atom could be nullified by too many positronium-proton collisions taking place at energies where the positron-transfer cross section is much smaller.

TABLE I. Positions of the cross-section maxima, the cross-section value at the maxima, and the energies at which the cross section falls to $\frac{1}{2}$ of its maximum value. (For the purposes of this table, the working cross section was the cross section including corrections for the $\bar{\text{H}}$ levels that were omitted from the UBA calculation.)

Initial Ps level	Maximum σ (πa_0^2)	Energy at maximum (eV)	Energy at half maximum (eV)
$1s$	14.6	6.0	>10
$2s$	185	0.55	3.5
$2p$	205	1.12	3.85
$3s$	740	0.73	1.32
$3p$	650	0.75	1.60
$3d$	800	0.75	1.84
$4s$	1230	0.36	0.72
$4p$	1560	0.36	0.74
$4d$	1180	0.40	0.98
$4f$	1890	0.36	0.95

ACKNOWLEDGMENT

The calculations reported herein were performed on a computing facility funded by the Australian Research Council.

[1] R. J. Hughes and B. I. Deutch, Phys. Rev. Lett. **69**, 578 (1992).
[2] R. J. Hughes, Nucl. Phys. A **558**, 605c (1993).
[3] M. Charlton, J. Eades, D. Horvath, R. J. Hughes, and C. Zimmerman, Phys. Rep. **241**, 67 (1994).
[4] B. L. Brown, L. Haarsma, G. Gabrielse, and K. Abdulah, Hyp. Int. **73**, 193 (1992).
[5] B. I. Deutch, F. M. Jacobsen, L. H. Andersen, P. Hvelplund, H. Knudsen, M. H. Holzscheiter, M. Charlton, and G. Laricchia, Phys. Scr. **T22**, 248 (1988).
[6] B. I. Deutch, L. H. Andersen, P. Hvelplund, F. M. Jacobsen, H. Knudsen, M. H. Holzcheiter, M. Charlton, and G. Laricchia, Hyp. Int. **44**, 271 (1988).
[7] B. I. Deutch, M. Charlton, M. H. Holzscheiter, P. Hvelplund, L. V. Jorgensen, H. Knudsen, G. Laricchia, J. P. Merrison, and M. R. Poulsen, Hyp. Int. **76**, 153 (1993).
[8] J. W. Humberston, M. Charlton, F. M. Jacobsen, and B. I. Deutch, J. Phys. B **20**, L25 (1987).
[9] J. Mitroy and A. T. Stelbovics, J. Phys. B **27**, 3257 (1994).
[10] J. Mitroy and A. T. Stebovics, Phys. Rev. Lett. **72**, 3495 (1994).
[11] J. Mitroy and K. Ratnavelu, J. Phys. B **28**, 280 (1995).
[12] A. Igarashi, N. Toshima, and T. Shirai, J. Phys. B **27**, L497 (1994).
[13] M. Charlton, Phys. Lett. A **143**, 143 (1990).
[14] J. W. Darewych, J. Phys. B **20**, 5917 (1987).
[15] S. N. Nahar and J. W. Wadehra, Phys. Rev. A **37**, 4118 (1988).
[16] J. Mitroy and A. T. Stelbovics, J. Phys. B **27**, L79 (1994).
[17] J. Mitroy, Aust. J. Phys. **46**, 751 (1993).
[18] J. Mitroy, D. C. Griffin, D. W. Norcross, and M. S. Pindzola, Phys. Rev. A **38**, 3339 (1988).
[19] J. Mitroy and D. W. Norcross, Phys. Rev. A **39**, 537 (1989).
[20] A. P. Mills and L. Pfeiffer, Phys. Rev. D **26**, 53 (1985).
[21] A. P. Mills, E. D. Shaw, R. J. Chichester, and D. M. Zuckerman, Phys. Rev. B **40**, 2045 (1989).